LL

CERN-CN 95-16

Presented at the SABER User Group Meeting
Brighton, UK, September 1995

CN 95/16

MAST Power Diode and Thyristor Models Including Automatic Parameter Extraction

Alan COURTAY

CERN,
European Laboratory for Particle Physics,
Geneva, Switzerland.

CERN LIBRARIES, GENEVA

CERN-CN-95-16

Abstract - Most power semiconductor models available in circuit simulators require physical input parameters, such as carrier lifetime, doping concentration or mobility. Unfortunately, these are generally not accessible to the user. The models described here use readily available databook parameters and automatically convert them into the physical constants of the underlying model equations. To achieve this conversion with the MAST modelling language, techniques are proposed to solve equations at the beginning of a simulation.

Relevant features found in existing models are combined to get an efficient power diode model in terms of accuracy, calculation speed and robustness. It includes junction capacitance, forward and reverse recovery phenomena. For all these effects, simulation results are compared with measurements. A new thyristor model featuring reverse recovery is also presented.

I. Introduction

CIRCUIT simulators, such as PSpice or Saber, generally provide two categories of power semiconductor device models. The first consists of simple models that basically represent semiconductor devices as switches. Although fast and easy to use, these models are insufficient for accurate simulations as they do not include internal effects such as diode reverse recovery.

The second category comprises more advanced models based on internal device physics. Their characterization is difficult since the required physical input constants (carrier life time, doping concentration, mobility, etc) are not readily available but must be estimated from measurable external parameters. Even if procedures for parameter extraction are described in related papers, this remains a nontrivial issue for the end-user. For this reason, the advanced models are mainly used by simulator manufacturers as the basis for building libraries of characterized models for commercial components.

The absence of advanced generic models with simple characterization was the motivation of the present work. Indeed, at the beginning of a circuit design, the application engineer typically explores concepts with different devices and topologies. At this level, such a model family would greatly help to study the influence of device features on the design, to identify the required device characteristics, and finally to choose the most appropriate components.

The power diode and thyristor models presented here use directly available databook parameters and automatically convert them into the physical constants of the underlying model equations. They are implemented in MAST, the Saber simulator modelling language. The diode model and its automatic parameter extraction are fully described. The dynamic features (junction capacitance, forward and reverse recovery) have been experimentally verified on Schottky and fast recovery diodes. On the basis of this diode model, a behavioural thyristor model was built.

II. Solving Equations during DC Analysis

Parameter extraction is easy if all internal constants can be expressed as explicit functions of the external parameters. But this is not always possible. In some cases, solving equations is the only way to calculate the internal constants. Let us consider such a case : the conductance g of a resistor model is related to an external parameter k through the following conversion equation :

$$g - \exp(-k.g) = 0 \qquad (1)$$

Clearly, the internal constant g can not be found analytically. Applied to this example, two general methods are now presented to solve such equations for parameter extraction at the beginning of a simulation.

The first method consists of performing the parameter extraction in the equations section of a MAST template [6]. The conversion equation is solved during the DC analysis by the Saber algorithms. Once the DC analysis has been performed, the solution is recorded in a state variable. The conversion equation then becomes redundant but is still to be solved at each time step of transient analysis. As this equation cannot be removed from the equations section, it is transformed into a simple artificial equation that reduces calculation time.

The template provided in figure 1 uses this method to extract the conductance *g* from the external parameter *k*. *eq* is a val variable that allows the equation expression to be changed between DC and transient analysis. During the DC analysis, the relevant equations to be solved are :

$$eq = g_\mathrm{var} - \exp(-k.g_\mathrm{var})$$
$$g_\mathrm{var} : eq = 0$$

The solution value *g_var* is then passed to a state variable *g_state*. The solution being stored, *g_var* no longer has any significance. After the DC analysis, *eq* is made equal to *g_var* and the equation

```
element template parameter_conversion p m = k
electrical p,m
number k
{
var nu g_var
val nu g_val
state nu g_state
val nu eq
when (dc_done) {g_state = g_val}
values {
    if (dc_domain) {
        g_val = g_var
        eq = g_var - exp(-k*g_var)
        }
    else    {
        g_val = g_state
        eq = g_var
        }
    }
equations {
    g_var : eq=0
    # The resistance template has to be rewritten :
    i(p->m)+=(v(p)-v(m))*g_val
    }
}
```

Fig. 1. Example of parameter conversion using the equations section

to be solved reduces to *g_var=0* :

$$eq = g_var$$
$$g_var : eq = 0$$

which is the simplest equation possible. Note that *g_state* is undefined during DC analysis and *g_var* is equal to zero during transient analysis. Only the val variable *g_val* is equal to the converted parameter during both DC and transient analysis.

This is the main disadvantage of the method. The value of a val variable cannot be passed as an argument to a lower level template. A template requiring the converted parameter as an input data can not be called from the netlist section. It has to be incorporated into the main template and adapted in order to accept the converted parameter as a val variable. If this task is easy for a resistance (fig.1), it becomes more problematic, if not impossible, for sophisticated encrypted models.

The second method avoids this inconvenience since the equation is solved in the parameters section. This method consists of calculating the first elements of a sequence that converges to the solution. To build this sequence, the equation has to be written in a form where the unknown variable g is expressed as a function of itself :

$$g = f(g) . \qquad (2)$$

In the graphical illustration of figure 2, the solution g appears as the crossing point between the curve y=f(x) and the line y=x. The sequence $\{g_n\}$ is defined by :

$$g_{n+1} = f(g_n) . \qquad (3)$$

As the sequence limit when n tends to infinity is the solution of equation (2), g can be approximated by g_n with n sufficiently large :

$$g = \lim_{n \to \infty} g_n . \qquad (4)$$

It is important to note that this method only works if the following condition on the function f(x) is satisfied :

$$-1 < \left. \frac{d[f(x)]}{dx} \right|_{x=g} < 1 . \qquad (5)$$

Appendix A explains why (5) is necessary. The choice of the first element g_0 can be arbitrary if this condition is verified for any value of x, but it is critical if condition (5) is only valid in the neighbourhood of g. To ensure the sequence convergence, g_0 then has to belong to this neighbourhood.

As the function f(x) depends on the external parameters, condition (5) may not be verified for all their possible values. If so, the equation then has to be written into another form (2) satisfying (5). This is the case with the conversion equation previously given in example :

$$g = \exp(-k.g) = f_1(g) . \qquad (6)$$

Under this form, condition (5) is only true for $k < \exp(1)$. For $k > \exp(1)$, equation (6) has to be written as follows :

$$g = -\frac{\ln g}{k} = f_2(g) . \qquad (7)$$

Then condition (5) applied to $f_2(x)$ is valid for $k > \exp(1)$ only.

The template given in figure 3 uses the described method to solve the conversion equation for any value of k. Note that the provided solution is a parameter variable, so the resistance template can directly be called from the netlist section.

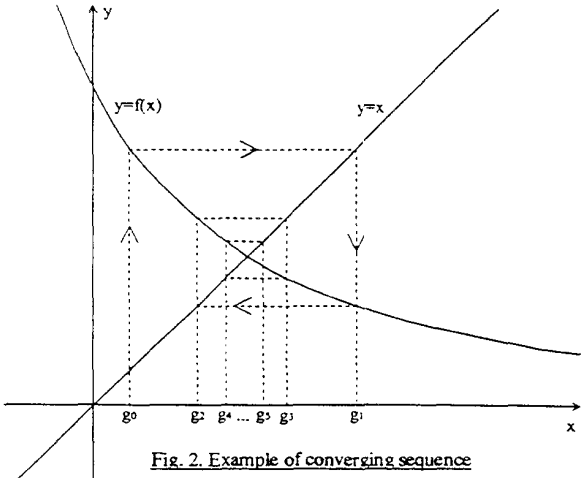


Fig. 2. Example of converging sequence

III. Diode Static Model

The diode static submodel is the basis to which all diode dynamic effects are going to be added. It consists of a contact resistance R_{on} in series with an ideal diode that represents the junction voltage V_j by the exponential law :

$$I_d = I_s . \left[\exp\left(\frac{V_j}{V_b} \right) - 1 \right] \qquad (8)$$

Some models ([2] and [4]) distinguish high-level injection, low-level recombination and emitter recombination effects by adding several ideal diodes in parallel using the same relationship (8) with different parameters I_s and V_b. This only has a small effect on the model characteristics near-zero. In the reverse-biased region of operation, the diode current remains constant, and above V_{on} , the curve is still governed by the series resistance. For power circuit simulation, one exponential law to describe the junction voltage gives sufficient accuracy and makes parameter extraction easier. The leakage current I_s and the series resistance R_{on} are directly

```
element template parameter_conversion p m =k
electrical p,m
number k
{
number g,g0,g1,g2,g3,g4,g5,g6,g7,g8,g9
parameters {
    if (k<exp(1)) {
        g0=0
        g1=exp(-k*g0)
        g2=exp(-k*g1)
        g3=exp(-k*g2)
        g4=exp(-k*g3)
        g5=exp(-k*g4)
        g6=exp(-k*g5)
        g7=exp(-k*g6)
        g8=exp(-k*g7)
        g9=exp(-k*g8)
        g=g9
        }
    if (k>exp(1)) {
        g0=0.5
        g1=-ln(g0)/k
        g2=-ln(g1)/k
        g3=-ln(g2)/k
        g4=-ln(g3)/k
        g5=-ln(g4)/k
        g6=-ln(g5)/k
        g7=-ln(g6)/k
        g8=-ln(g7)/k
        g9=-ln(g8)/k
        g=g9
        }
    }
# Resistance template directly called from netlist section
r.r p m =1/g
}
```

Fig. 3. Solving the conversion equation in the parameters section

provided by the diode I-V characteristics (fig.4). The junction barrier potential V_b is also easily extracted :

$$V_b = \frac{V_{on} - R_{on}}{\ln\left(1+\frac{1}{I_s}\right)} \qquad (9)$$

where V_{on} corresponds to a current of 1 Amp through the diode.

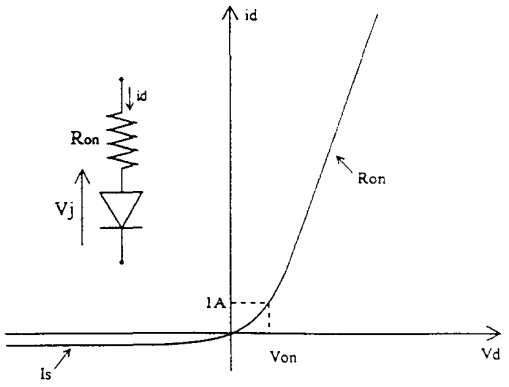


Fig. 4. Diode DC Model

IV. Diode Reverse Recovery

Reverse recovery is the most important diode dynamic effect for power circuit designers as it introduces overvoltages and high power dissipation. The phenomenon occurs when a forward biased diode is turned off rapidly. The excess charge, stored in its lightly-doped region during conduction, takes some time to be removed. During this time, the diode remains conducting and a reverse current can flow through it. It then works as a short circuit whereas it should be an open circuit.

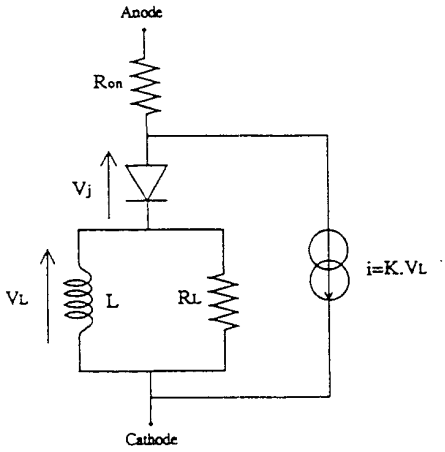


Fig. 5. Diode reverse recovery model

Based on a macro-modelling approach, the reverse recovery submodel proposed by [1] is extremely easy to implement since it simply consists of a resistance, an inductance and a controlled current source (fig.5). Note that the DC representation in the original model [1], composed of a binary resistance Ron / Roff in series with a constant voltage source Vj, is not satisfactory since the diode works as a generator under zero-bias. It was thus replaced by the DC submodel of the previous section.

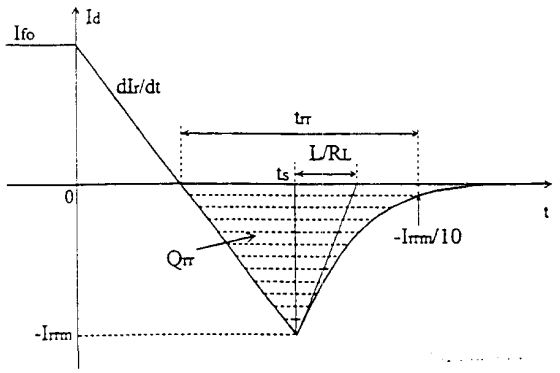


Fig. 6. Diode current turn-off waveform

Turned off with an inductive load, the circuit model (fig.5) provides the typical diode reverse current waveform of figure 6. For $t < ts$, the ideal diode conducts and the external circuit determines the diode current. As I_d linearly decreases, the constant negative voltage across L commands a constant reverse current Irrm through the controlled source. At time $t = ts$, I_d reaches $-$ Irrm. The ideal diode then gets blocked since its current has decreased to zero. After $t > ts$, the ideal diode can be regarded as an open switch. The subcircuit R_L // L now acts independently of the

external circuit, and imposes an exponential current decrease with a time constant L / R_L :

$$I_d(t) = I_{rrm}.\exp\left[-\frac{R_L.(t-t_s)}{L}\right] \quad (10)$$

In fact, the model only depends on two intrinsic parameters : L / R_L and K (the coefficient of the voltage controlled current source). As most power diode databooks provide Irrm, trr and Qrr for specified Ifo and dIr/dt conditions, L / R_L and K have been related to these external parameters. The time constant is given by (11) and K is obtained by solving equation (12).

$$\frac{L}{R_L} = \frac{1}{\ln 10}\left(t_{rr} - I_{rrm}\left(\frac{dI_r}{dt}\right)^{-1}\right) \quad (11)$$

$$K = \frac{I_{rrm}}{L}\left(\frac{dI_r}{dt}\right)^{-1}.\left[1-\exp\left(\frac{-I_{Fo}-I_{rrm}}{L\dfrac{dI_r}{dt}\left(K+\dfrac{1}{R_L}\right)}\right)\right]^{-1} = f(K) \quad (12)$$

A degree of liberty exists between L and R_L , so the inductance is arbitrarily set equal to 10 pH. This very low value makes V_L negligible compared to V_j. With $K >> 1$, the inductance acts as a probe measuring dIr/dt for the controlled current source. L being fixed, R_L can be directly deduced from (11). Equation (12) is solved in the parameters section, using the second method described in section II. Note that the corresponding function f(K) is guaranteed to verify condition (5) for any acceptable values of the reverse recovery input parameters.

These parameters are initially checked to be valid by the template. In particular, the following conditions, imposed by the reverse current geometry (fig.6), must be respected :

$$Q_{rr} < \frac{t_{rr}^2}{2}.\frac{dI_r}{dt} \quad (13)$$

$$I_{rrm} < t_{rr}.\frac{dI_r}{dt} \quad (14)$$

$$Q_{rr} > \frac{I_{rrm}^2}{2}\left(\frac{dI_r}{dt}\right)^{-1} \quad (15)$$

If not, the internal constants cannot be calculated, and reverse recovery is removed from the model (as well as forward recovery). Note that once the turn-off conditions Ifo and dIf/dt are given, only two parameters out of Irrm, trr and Qrr are needed to define the current turn-off waveform, the third one being redundant. The diode template is implemented to handle any combination of two parameters, but if all three are provided, Irrm and trr only are used to calculate R_L and K. The geometric relationships linking Irrm, trr and Qrr are the following :

$$\left(\frac{1}{2}-\frac{1}{\ln 10}\right)\left(\frac{dI_r}{dt}\right)^{-1} I_{rrm}^2 + \frac{t_{rr}}{\ln 10} I_{rrm} - Q_{rr} = 0 \quad (16)$$

$$t_{rr} = \frac{\ln 10}{I_{rrm}}\left[Q_{rr} - \left(\frac{1}{2}-\frac{1}{\ln 10}\right)\left(\frac{dI_r}{dt}\right)^{-1} I_{rrm}^2\right] \quad (17)$$

To validate the model experimentally, a fast recovery diode was tested in the chopper circuit of figure 7. In order to get steep current slopes, the parasitic inductance L_p was reduced to 130 nH by an optimized geometric circuit design. Figure 8 shows the comparison between measured and simulated turn-off waveforms.

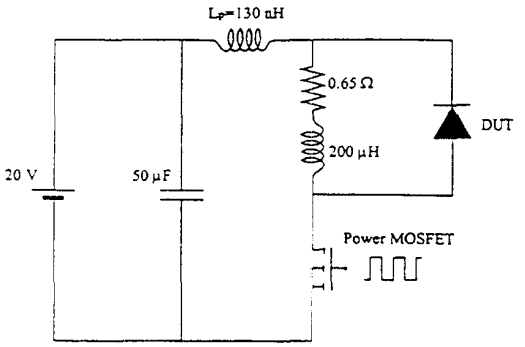


Fig. 7. Chopper circuit for measuring diode switching transients

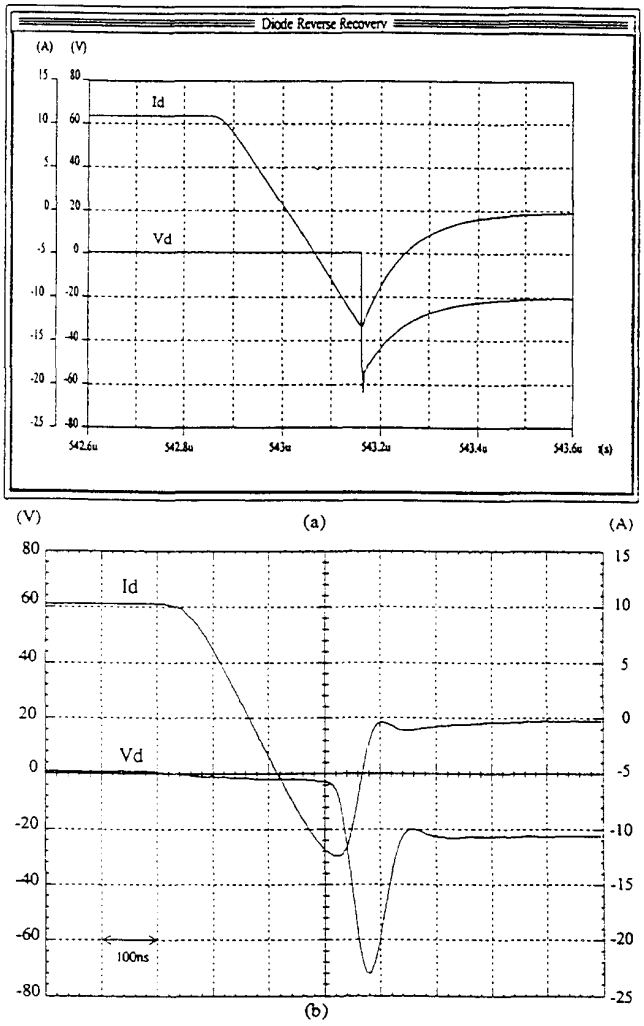
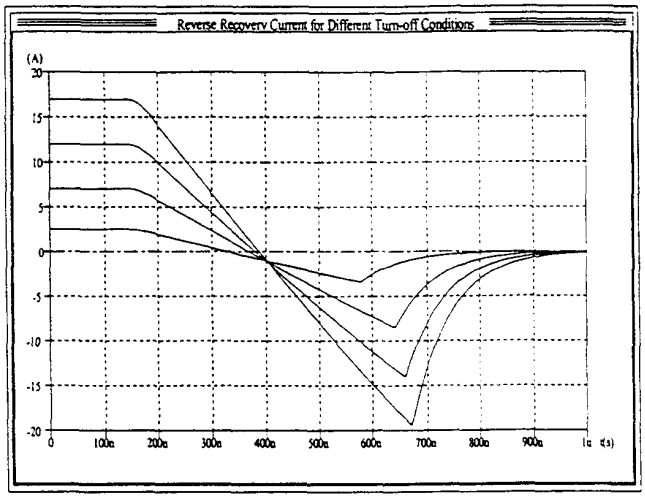
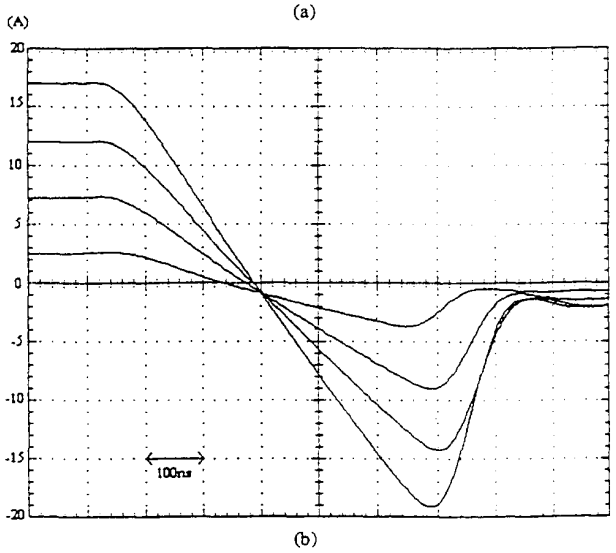


Fig. 8. Simulated (a) and measured (b) turn-off waveforms of the Thomson fast recovery diode ESM 244-100

Macro-models are often considered to have a narrow range of accuracy, but the reverse recovery circuit model remains valid over a wide range of operating conditions. Whereas its internal parameters have been calculated for a given turn-off waveform, it still gives good agreement with measurement when simulated in different blocking conditions (fig.9). Moreover, this model is shown in Appendix B to be strictly equivalent to the micro-model developed by Lauritzen and Ma [2]. Table 1 gives the correspondences between both models. The internal constants and currents of the circuit model [1] can thus be related to physical constants and variables such as transit time, carrier lifetime or excess charge in the diode lightly-doped region.



(a)



(b)

Fig. 9. Simulated (a) and measured (b) reverse recovery currents in different blocking conditions

TABLE I

Equivalent expressions for Lauritzen's micro-model parameters and variables in the circuit model of figure 5 (cf. Appendix B)

$$\tau = KL\left(1+\frac{1}{R_L K}\right) \qquad q_m(t) = KL\left(1+\frac{1}{R_L K}\right) i_L(t)$$

$$T_m = \frac{L}{R_L}\left(1+\frac{1}{R_L K}\right) \qquad q_e(t) = KL\left(1+\frac{1}{R_L K}\right)^2 (i_{R_L}(t) + i_L(t))$$

$$I_s^* = I_s\left(1+\frac{1}{R_L K}\right) \qquad V_t^* = \frac{V_b}{2}$$

V. Diode Forward Recovery

The forward recovery phenomenon occurs when the diode switches from its nonconducting to its conducting state. During this transient, a voltage overshoot develops across the diode because of initial low conductivity in the lightly-doped region. This conductivity rapidly increases due to the increased concentration of injected carriers. As this concentration is established by the forward current, the voltage overshoot peak value V_{fp} and its corresponding time t_{fp} mainly depend on the rate of current rise dIf/dt.

The voltage overshoot at turn-on can be modelled by a dependent voltage source V_m in series with the reverse recovery circuit. The analytical description of V_m was proposed by Batard et al. in their power diode model [3]. Derived from Lauritzen's model, it uses the same equations for reverse recovery, but presents a more satisfactory forward recovery than in [2]. The improved forward recovery submodel consists of the following equations :

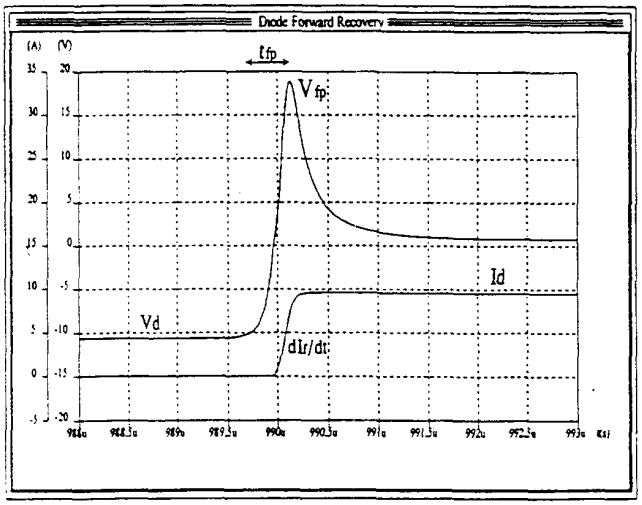
$$\frac{dq_m}{dt}(t) \geq 0 : \quad V_m(t) = V_1(t) - V_2(t) \tag{18}$$

$$V_1(t) = \frac{I_d^2(t)}{\frac{q_e^2(t)}{\beta\tau} + \frac{I_d(t)}{R_0}}$$

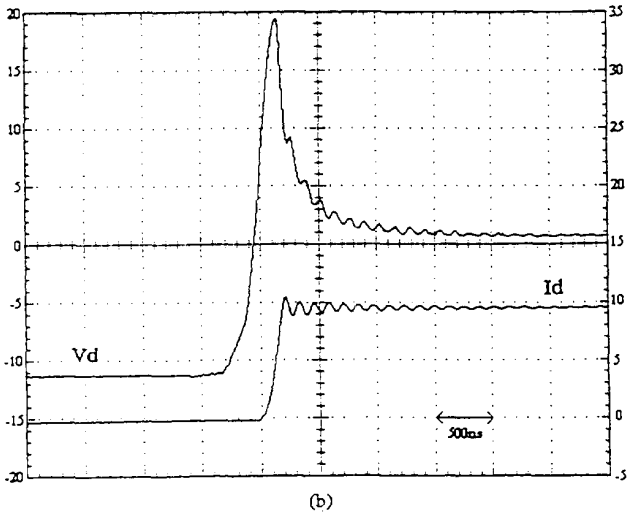
$$V_2(t) = \frac{I_d(t)}{\frac{\tau}{\beta}\left(1+\frac{T_m}{\tau}\right)^2 I_d(t) + \frac{1}{R_0}}$$

$$\frac{dq_m}{dt}(t) < 0 : \quad V_m(t) = 0 . \tag{19}$$

Using the equivalence between models [1] and [2] (table 1), the above equations are easily adapted to the reverse recovery circuit.



(a)



(b)

Fig. 10. Simulated (a) and measured (b) forward recovery waveforms

Equation (18) includes four physical parameters : τ (carrier life-time), T_m (transit time), R_0 (initial resistance in the lightly-doped region) and β (a parameter depending on various geometrical and physical parameters of the diode). As τ and T_m are determined by a reverse recovery current waveform, R_0 and β are the only free parameters to characterize the forward recovery voltage. They are calculated to give the correct values of V_{fp} and t_{fp} for a given dIf/dt. Appendix C describes a complete procedure to automatically extract R_0 and β from the external parameters dIf/dt, V_{fp} and t_{fp}. This procedure, only partially found by [3], uses the first method described in section II for solving equations in the DC analysis. As shown in figure 10, the agreement between the simulated and measured turn-on waveforms of the Thomson diode in the chopper circuit is excellent. Moreover the model is shown in [3] to remain valid over a wide range of dIf/dt conditions.

VI. Diode Junction Capacitance

The last dynamic effect to be added to the diode model is due to space charge regions of opposite signs that develop on both sides of the junction. The corresponding capacitance depends on the width of these regions which in turn depends on the applied voltage. This effect is particularly pronounced in Schottky diodes where large oscillations at turn-off due to their high junction capacitances mask their low reverse recovery currents.

An accurate description of the junction capacitance is given by :

$$V_j < 0 \quad : \quad C(V_j) = \frac{C_0}{\left(1 - \frac{V_j}{V_b}\right)^m} \tag{20}$$

$$V_j > 0 \quad : \quad C(V_j) = C_0\left(1 + m\frac{V_j}{V_b}\right) \tag{21}$$

The gradient factor m depends on doping profiles and typically ranges from 0.3 to 0.5. C_0 is the junction capacitance for zero bias. The two relationships needed to identify these parameters are given by two points (V_1 , C_1) and (V_2 , C_2) extracted from a standard C-V plot. C_0 and m are calculated in the template as follows :

$$m = \frac{\ln\left(\frac{C_1}{C_2}\right)}{\ln\left(\frac{1+\frac{V_2}{V_b}}{1+\frac{V_1}{V_b}}\right)} \approx \frac{\ln\left(\frac{C_1}{C_2}\right)}{\ln\left(\frac{V_2}{V_1}\right)} \tag{22}$$

$$C_0 = C_1.\left(1+\frac{V_1}{V_b}\right)^m \approx C_1.\left(\frac{V_1}{V_b}\right)^m \tag{23}$$

If only one point (V_1 , C_1) is provided by the user, the gradient factor is set equal to the average value 0.4, and C_0 is calculated by using (23).

The junction capacitance is implemented in MAST as a voltage controlled current source. The current through C_j is defined as :

$$I_c(V_j) = \frac{d}{dt}\int C(V_j)dV_j \tag{24}$$

which leads to :

$$V_j < 0 \quad : \quad I_c(V_j) = \frac{d}{dt}\left[\frac{C_0.V_b}{(m-1)}\left(\left(1-\frac{V_j}{V_b}\right)^{1-m} - 1\right)\right] \tag{25}$$

$$V_j > 0 \quad : \quad I_c(V_j) = \frac{d}{dt}\left[C_o.V_j.\left(1+\frac{m.V_j}{2V_b}\right)\right] \tag{26}$$

The turn-off behaviour of a Schottky diode was studied in the chopper circuit. Figure 11 shows measured and simulated voltage waveforms at turn-off. The oscillations are due to the resonance between the junction capacitance of the diode and the parasitic inductance of the circuit. Note that these oscillations are not purely sinusoidal. As the voltage oscillates, the junction capacitance changes, which slightly affects the resonant frequency.

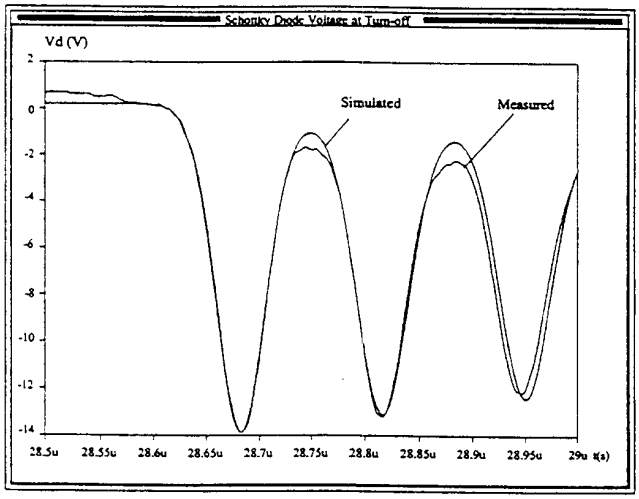


Fig. 11. Voltage turn-off waveforms of the Motorola Schottky diode MBR30045CT

Equation (20) was experimentally verified by measuring the junction capacitance for different reverse voltages (fig.12). The parasitic inductance of the test circuit was estimated as 130 nH by placing known capacitors in parallel to the diode. The junction capacitance values were then deduced from the oscillation period T using :

$$C_j = \frac{1}{L_p}\left(\frac{T}{2\pi}\right)^2 \tag{27}$$

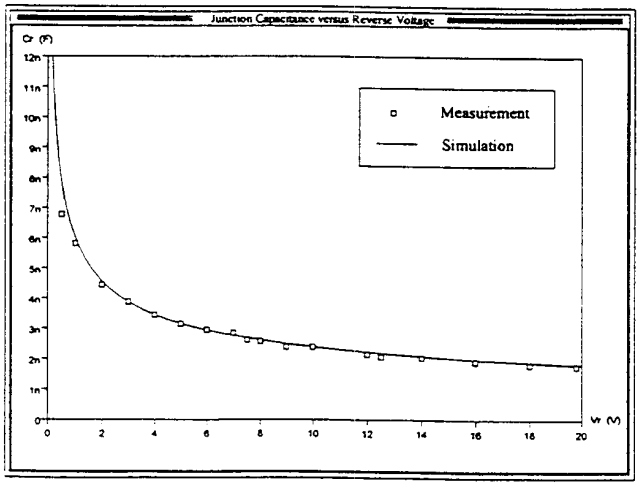


Fig. 12. Schottky diode junction capacitance

The diode model is now complete (fig.13). Its input parameters are listed in table 2.

TABLE II

Diode input parameters

Features	Parameters
I-V Characteristics	Ron, Von, Is
Reverse Recovery	Ifo, dIr/dt, Irrm, trr, Qrr
Forward Recovery	dIr/dt, Vfp, tfp
Junction Capacitance	C_1, V_1, C_2, V_2

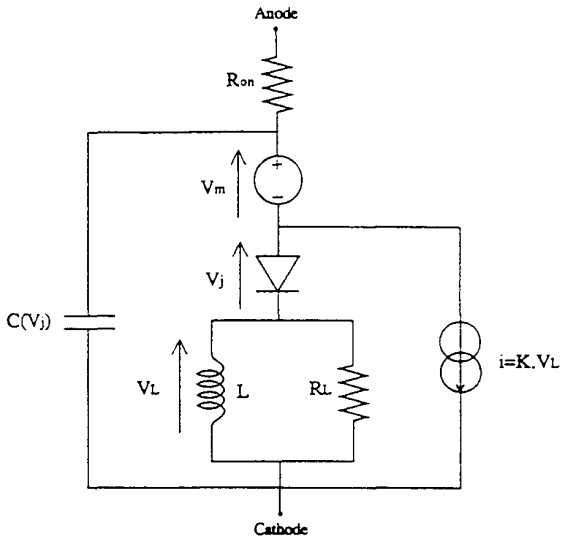


Fig. 13. Complete power diode model

Because of its modular structure, the diode model can be used with different degrees of accuracy. By assigning zero to some input parameters, the user is able to specify the features to be retained for his simulation. For example, in the first approach of a design, the DC submodel may provide sufficient accuracy with low computational time. When more insight is needed, dynamic effects can then be added one by one. This gradual approach into complexity makes the model very convenient for the user.

VII. Derived Thyristor Model

Thyristors (or SCRs) are widely used in power switching networks due to their high power-handling capabilities. They can be regarded as diodes that turn-on with a gate terminal current pulse. When turning off, the thyristor presents a reverse recovery phenomenon like the power diode.

A thyristor model with reverse recovery is proposed by [5] following the same micro-modeling approach as for their diode [2]. The analog gate obliges the user to add a triggering circuit for each component. If the simulated circuit has a large number of thyristors, the simulation complexity is greatly increased without providing more accuracy in the main circuit response.

The new thyristor model presented here has a digital gate and also includes reverse recovery. The model is directly derived from the diode reverse recovery circuit by replacing the contact resistance with a module that realizes the thyristor static properties (fig.14). This *scr_logic* module is basically a binary resistance R_{on} / R_{off} controlled by a digital gate. When the thyristor is in the off-state under positive voltage, R_{off} blocks the current that would flow through the diode. In the on-state, R_{on} is the contact resistance as in the diode model.

The transition R_{off} to R_{on} occurs when V_{ak} is positive and the gate active. It will also happen if V_{ak} exceeds the break-over voltage V_{bo}. The turn-on time t_f is the parameter to be adjusted in order to reproduce accurately turn-on transients and switching losses.

The thyristor remains in the on-state until it gets reverse biased for sufficient time to have most of its excess charge q_m removed from the lightly-doped region. The parameter t_q is the minimum time interval for which V_{ak} must be maintained negative to guarantee thyristor turn-off. As t_q is measured for given blocking conditions (I_0, dIr/dt, Irrm...), its range of validity is quite narrow, but it can be related to a critical amount of stored charge q_{mc} that is independent of these conditions. This critical charge turns out to be the relevant internal parameter to command thyristor turn-off : the transition R_{on} to R_{off} is triggered when q_m has decreased to q_{mc} , or equivalently when the current through the inductance L has decreased to the corresponding critical current i_{Lc} (table 1 shows the correspondence between i_L and q_m). This critical current, calculated from t_q and the specified reverse current waveform, is given by equation (28).

$$i_{Lc} = \frac{I_{rrm}}{R_L.K}.\exp\left[-\frac{R_L}{L}\left(t_q - \frac{dt}{dI_r}.I_{rrm}\right)\right] \qquad (28)$$

The thyristor input parameters are listed in table 3. The parameter init_state allows the thyristor initial state to be specified, provided V_{ak} is positive at the beginning of the simulation. For simplicity, the junction capacitance is a constant C but it can be easily replaced by the diode junction capacitance submodel. Note that this capacitance helps convergence in the simulation of thyristor Graetz bridges.

TABLE III

Thyristor input parameters

Features	Parameters
I-V Characteristics	Ron, Von, Is, init_state
Reverse Recovery	Ifo, dIr/dt, Irrm, trr, Qrr
Junction Capacitance	C
Turn-on Transient	tf
Critical Turn-on	tq, Vbo

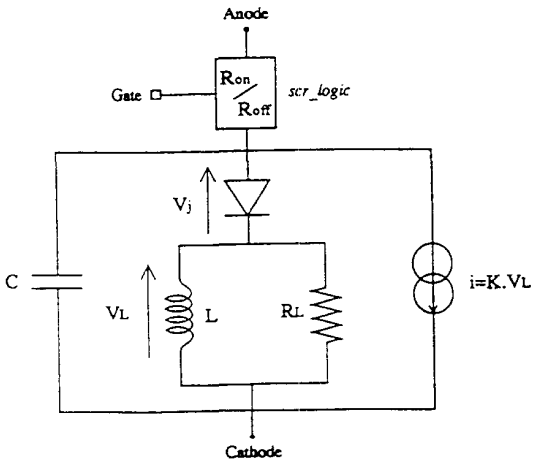


Fig. 14. Thyristor model

VIII. Conclusion

Based on general methods for solving equations at the beginning of a simulation, the concept of automatic parameter extraction goes beyond the scope of semiconductor modelling. However, the limits of this concept must be acknowledged. The model equations have to be rearranged in a way that allows every internal constant to be related to measurable quantities. Some advanced models, such as the IGBT model by Hefner et al.[7], have internal constants so closely tied and entangled in a set of complex equations that it is nearly impossible to establish a systematic procedure for parameter extraction. The model characterization can only be processed by extensive measurements on an experimental bench and parameter fitting by means of a computer.

However, the examples given in this paper show that it is possible to make accurate models that can be easily characterized by the end-user. They have been succesfully used at CERN in the simulation of choppers, pole inverters and Graetz bridges.

APPENDIX A

Necessary condition to solve an equation in the parameters section

Let $\{g_n\}$ be a sequence defined as follows :

$$g_{n+1} = f(g_n). \tag{A1}$$

The sequence convergence implies that

$$|g_{n+2} - g_{n+1}| < |g_{n+1} - g_n| \tag{A2}$$

or equivalently,

$$|f(g_{n+1}) - f(g_n)| < |g_{n+1} - g_n| \tag{A3}$$

The above inequality is guaranteed if we have

$$\left|\frac{df}{dx}\right| < 1 \tag{A4}$$

In other words, the described method to solve g=f(g) applies if the curve y=f(x) cuts the line y=x with a slope in the interval [-1,1]. Figure 15 exhibits a function f(x) that does not satisfy (A4) and which sequence $\{g_n\}$ diverges.

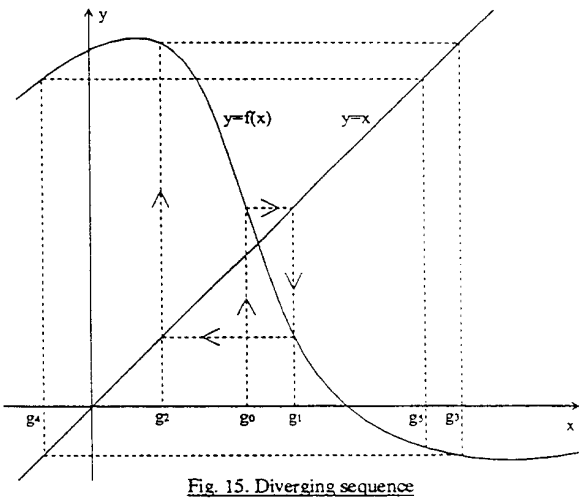


Fig. 15. Diverging sequence

APPENDIX B

Equivalence between Circuit Model [1] and Micro-Model [2]

The following set of equations describes the DC and reverse recovery behaviours of Lauritzen's diode model [2] :

$$I_d(t) = \frac{q_e(t) - q_m(t)}{T_m} \tag{B1}$$

$$I_d(t) = \frac{dq_m}{dt}(t) + \frac{q_m}{\tau}(t) \tag{B2}$$

$$q_e(t) = I_S^*.\tau\left[\exp\left(\frac{V_j(t)}{2V_t^*}\right) - 1\right] \tag{B3}$$

$$V_d(t) = V_j(t) + R_{on}.I_d(t) \tag{B4}$$

where $q_e(t)$ is the junction charge varaible,
$q_m(t)$ is the charge in the lightly-doped region,
T_m is the transit time,
τ is the carrier lifetime,
I_s^* is the diffusion leakage current,
V_j is the junction voltage,
V_t^* is the junction barrier potential,
R_{on} is the internal series resistance.

Referring to figure 4, equation (B4) is clearly valid for the circuit model. (B3) will now be compared to equation (8). Under DC conditions, (B1) and (B2) give

$$q_e = (\tau + T_m).I_d \tag{B5}$$

By substitution into (B3), we get

$$I_d = \frac{I_s^*.\tau}{(T_m + \tau)}\left[\exp\left(\frac{V_j}{2V_t^*}\right) - 1\right] \tag{B6}$$

which is equivalent to (8).

Regarding reverse recovery, the models are also strictly equivalent since they are ruled by the same equations. As a demonstration, the micro-model equations (B1) and (B2) are going to be derived from the circuit model. Referring to figure 5, Kirchhoff's current law gives

$$i_d = i + i_{R_L} + i_L \tag{B7}$$

or equivalently,

$$i_d = K.V_L + \frac{V_L}{R_L} + i_L \tag{B8}$$

$$i_d = KL\left(1 + \frac{1}{R_L K}\right)\frac{di_L}{dt} + i_L \tag{B9}$$

Comparing equation (B9) with (B2) gives the relationships linking τ and q_m to the parameters and variables of the circuit model (table 1). Transforming again equation (B7) :

$$i_d = R_L K\left[i_{R_L} + \frac{i_{R_L}}{R_L K} + \frac{i_L}{R_L K}\right] \tag{B10}$$

$$i_d = R_L K\left[\left(1 + \frac{1}{R_L K}\right).\left(i_{R_L} + i_L\right) - i_L\right] \tag{B11}$$

$$i_d = \frac{KL\left(1+\frac{1}{R_L K}\right)^2\left(i_{R_L}+i_L\right) - KL\left(1+\frac{1}{R_L K}\right)i_L}{\frac{L}{R_L}\left(1+\frac{1}{R_L K}\right)} \qquad \text{(B12)}$$

By comparing (B12) with (B1), we obtain the equivalent expressions for T_m and q_e in the circuit model.

APPENDIX C

Automatic Extraction of the Forward Recovery Parameters R_0 and β.

We assume that the diode current slope dIf/dt is constant at turn-on :

$$I_d(t) = \frac{dI_f}{dt}.t \qquad \text{(C1)}$$

The charge $q_m(t)$ can then be found by solving equation (B2) with the boundary condition $q_m(0)=0$:

$$q_m(t) = \tau^2 \frac{dI_f}{dt}\left[\exp\left(\frac{-t}{\tau}\right)+\frac{(t-\tau)}{\tau}\right] \qquad \text{(C2)}$$

Using (B1), $q_e(t)$ at turn-on is defined as :

$$q_e(t) = \tau \frac{dI_f}{dt}\left[\left(1+\frac{T_m}{\tau}\right)t - \tau\left(1-\exp\left(\frac{-t}{\tau}\right)\right)\right] \qquad \text{(C3)}$$

The voltage drop V_m becomes :

$$V_m(t) = V_1(t) - V_2(t)$$

$$V_1(t) = \frac{t}{\frac{\tau}{t\beta}\left[\left(1+\frac{T_m}{\tau}\right)t - \tau\left(1-\exp\left(\frac{-t}{\tau}\right)\right)\right]^2 + \frac{dt}{dI_f}\frac{1}{R_0}} \qquad \text{(C4)}$$

$$V_2(t) = \frac{t}{\frac{\tau}{\beta}\left(1+\frac{T_m}{\tau}\right)^2 t + \frac{dt}{dI_f}\frac{1}{R_0}} \qquad \text{(C5)}$$

At time t_{fp}, V_m attains its maximum value V_{fp}. We thus have to solve the system

$$\begin{cases} V_m(t_{fp}) = V_{fp} \\ \dfrac{dV_m}{dt}(t_{fp}) = 0 \end{cases}$$

By using the polynomial expansion

$$\exp\left(-\frac{t}{\tau}\right) \approx 1 - \frac{t}{\tau} + \frac{t^2}{2\tau^2}$$

we obtain a simplified expression for V_1

$$V_1(t) = \frac{t}{\frac{T_m}{\beta\tau}(T_m+t)t + \frac{dt}{dI_f}\frac{1}{R_0}} \qquad \text{(C6)}$$

The system to be solved now becomes

$$V_{fp} = \frac{t_{fp}}{\frac{T_m}{\beta\tau}(T_m+t_{fp})t_{fp} + \frac{dt}{dI_f}\frac{1}{R_0}} - \frac{t_{fp}}{\frac{\tau}{\beta}\left(1+\frac{T_m}{\tau}\right)^2 t_{fp} + \frac{dt}{dI_f}\frac{1}{R_0}} \qquad \text{(C7)}$$

$$\frac{\frac{dt}{dI_f}\frac{1}{R_0} - \frac{t_{fp}^2.T_m}{\beta\tau}}{\left[\frac{T_m}{\beta\tau}(T_m+t_{fp})t_{fp} + \frac{dt}{dI_f}\frac{1}{R_0}\right]^2} = \frac{\frac{dt}{dI_f}\frac{1}{R_0}}{\left[\frac{\tau}{\beta}\left(1+\frac{T_m}{\tau}\right)^2 t_{fp} + \frac{dt}{dI_f}\frac{1}{R_0}\right]^2} \qquad \text{(C8)}$$

Using (C7), β can be expressed as a function of R_0 :

$$\frac{1}{\beta} = \frac{-\left[\frac{(a-c)}{V_{fp}}t_{fp} + \frac{(ab+bc)}{R_0}\right] + \sqrt{\Delta}}{2ac} \qquad \text{(C9)}$$

with $a = \frac{T_m}{\tau}(T_m+t_{fp})t_{fp}$ (C10)

$$b = \frac{dt}{dI_f} \qquad \text{(C11)}$$

$$c = \tau\left(1+\frac{T_m}{\tau}\right)^2 t_{fp} \qquad \text{(C12)}$$

$$\Delta = \left[\frac{(a-c)}{V_{fp}}t_{fp} + \frac{(ab+bc)}{R_0}\right]^2 - 4ac\frac{b^2}{R_0^2} \qquad \text{(C13)}$$

By substituting (C9) into (C8), we now get one equation with one unknown, R_0. (C8) is solved in the equations section under the following form :

$$0 = \left(-\frac{d}{\beta}+\frac{b}{R_0}\right)\left(\frac{c}{\beta}+\frac{b}{R_0}\right)^2 - \frac{b}{R_0}\left(\frac{a}{\beta}+\frac{b}{R_0}\right)^2 \qquad \text{(C14)}$$

with $d = \frac{T_m}{\tau}.t_{fp}^2$ (C15)

To avoid division by zero, the equation is solved by choosing $1/R_0$ as the corresponding var variable.

ACKNOWLEDGEMENTS

I would like to thank John EVANS for his useful discussions when writing this paper.

I am grateful to Rudi ZURBUCHEN, who initiated this research, for having proposed it to me.

I also wish to thank Frederick BORDRY who followed this work from the technical point of view and gave me his support with measurement.

REFERENCES

[1] C. BATARD - "Interactions Composants-Circuits dans les onduleurs de tension - Caracterisation - Modelisation - Simulation", Ph.D dissertation, Institut National Polytechnique de Toulouse, 1992.

[2] C.L. MA, P.O. LAURITZEN - "A Simple Power Diode Model with Forward and Reverse Recovery", *IEEE Power Electronics Specialists Conference*, pp. 411-415, 1991.

[3] C. BATARD, D.M .SMITH, H. ZELAYA, C.J. GOODMAN - "New High Power Diode Model with both Forward and Reverse Recovery", *IEE Conference Publication on Power Electronics and Variable-Speed Drives*, No. 399, pp. 447-452, October 1994.

[4] H.A. MANTOOTH, R.G. PERRY, J.F. DULIERE - "A Unified Diode Model for Circuit Simulation", *IEEE Power Electronics Specialists Conference*, Vol. 2, pp. 851-857, Atlanta, June 1995.

[5] C.L. MA, P.O. LAURITZEN - "A Physically-based Lumped-Charge SCR Model", *IEEE Power Electronics Specialists Conference*, pp. 53-59, Seattle, June 1993.

[6] ANALOGY, Inc. - "Guide to Writing Templates", Appendix A (Template Sections), Beaverton, USA, August 1993.

[7] A.R. HEFNER, D.M. DIEBOLT - "An experimentally verified IGBT model implemented in the Saber circuit simulator", *IEEE Power Electronics Specialists Conference*, Cambridge, MA, June 1991.